# Spatiotemporal Patterns, Drivers, and Socio-Ecological Synergies of Agrivoltaics in China

Xiaohan Li, Ruishuang Zhu, Ran Li, Yinghe Wang*

Suihua University, Suihua, 15200, China

*wyh971006@foxmail.com

**Abstract.** Based on panel data from 370 prefecture-level cities and 7 agricultural types during 2010-2022, this study systematically analyzes the temporal evolution, type-structure, driving factors, and regional comprehensive benefits of agrivoltaic projects. The innovations are: (1) constructing a four-dimensional framework of "temporal dynamics-type structure-driving attribution-comprehensive benefit"; (2) introducing Random Forest to quantify the impact of different factors on installed capacity; (3) designing a Comprehensive Benefit Index covering carbon reduction, employment generation, and economic output, overcoming the limitation of single-capacity indicators. Results show that national new capacity exhibits a "steep-rise then high-level fluctuation" pattern, with crop and fishery types dominating, and Qianxinan AP ranking highest in comprehensive benefits. This study provides data support for optimizing agrivoltaic project layout and benefit assessment.

**Keywords:** Agrivoltaics; Spatiotemporal Evolution; Random Forest; Comprehensive Benefit Index; Prefecture-Level Panel Data

## 1 Introduction

Agrivoltaics, a dual-use land management strategy that spatially couples photovoltaic power generation with agricultural production, is widely regarded as a strategic pathway to address the dual challenges of energy security and food security. As the world's largest and fastest-growing photovoltaic market, China's cumulative installed PV capacity reached 1 TW by the end of 2024, with PV power generation accounting for 21% of the nation's total installed capacity [1]. Against this backdrop, the integration of "PV+agriculture" has become a critical lever for advancing China's energy transition and rural revitalization.

At the micro-environmental level, the installation of PV panels alters the distribution of light and thermal resources within farmland. Zhang et al. (2023), investigating an open-field agrivoltaic system in eastern China, revealed that PV panel shading creates significant horizontal and vertical gradients in the light environment, with summer transmittance from ground level to crop canopy height ranging between 20.7% and 61.5% [2]. Geng et al. (2026) further demonstrated, through field experiments and numerical simulations, that tracking agrivoltaic arrays exhibit pronounced

© The Author(s) 2026

B. P. Siba et al. (eds.), *Proceedings of the 2026 5th International Conference on Public Service, Economic Management and Sustainable Development (PESD 2026)*, Advances in Economics, Business and Management Research 411,
https://doi.org/10.2991/978-94-6239-825-2_7

spatiotemporal heterogeneity across key solar terms, with average light capture rates of 46.1% and 43.2% at under-panel and inter-panel measurement points, respectively, and wheat yield reductions of 11.5% and 6.6% compared to open-field controls [3]. Wu et al. (2025) focused on PV module layout density as a critical design parameter, confirming through gradient experiments that module density significantly affects the micro-environment, yield, and nutritional quality of sweet potato [4]. While these micro-scale studies have elucidated the response mechanisms of the photothermal environment within agrivoltaic systems, they are predominantly site-specific experiments and lack systematic quantitative assessments at the macro scale.

At the methodological level, multimodal remote sensing image matching techniques provide critical support for the spatial identification and change monitoring of agrivoltaic power stations. Due to significant nonlinear radiation distortions (NRD) and geometric deformations between images acquired by different sensors, conventional matching methods face substantial challenges. In recent years, researchers have proposed a series of robust matching methods: Zhu et al. (2023) proposed $R_2FD_2$, achieving fast and robust matching through a multichannel autocorrelation of log-Gabor detector and a rotation-invariant maximum index map of log-Gabor descriptor [5]; Tu et al. (2022) proposed RI-LPOH, constructing a rotation-invariant local phase orientation histogram based on the maximum index map (MIM) and 2D matrices, achieving rotational invariance without separately estimating the principal orientation [6]; Zhang et al. (2025) proposed GLIFT, employing a global-to-local search strategy and a 3-D descriptor structure to effectively address scale and rotation variations in multimodal remote sensing images[7]; Fan et al. (2024) proposed GLS-MIFT, based on first-order Gaussian steerable filters and an adaptive partitioning descriptor, achieving matching performance superior to mainstream methods such as SIFT and RIFT on large-scale multimodal datasets[8]; Geng et al. (2025) proposed MIRRIFT, specifically designing a multi-resolution dimensional feature point extraction strategy and an enhanced Log-Gabor descriptor to address rotation and resolution variations [9]. Time et al. (2024), from the perspective of "conservation agrivoltaics," emphasized the importance of integrating well-characterized conservation agriculture management practices into agrivoltaic systems to enhance environmental sustainability and climate resilience [10].

In summary, the innovations of this study are threefold: (1) it provides the first systematic, full-type, long-term quantitative assessment of agrivoltaic projects in China at the prefecture-city scale; (2) it employs a Random Forest model to preliminarily identify potential driving factors of installed capacity, revealing the relative importance of temporal trends and type structures among the limited internal features considered; and (3) it constructs a comprehensive benefit index encompassing four dimensions—carbon reduction, elderly and youth employment generation, and economic output—providing a quantitative tool for regional comparison and optimized layout of agrivoltaic projects.

# 2 Data Sources and Methods

## 2.1 Data Sources and Preprocessing

Raw data were obtained from the Vectorized Agrivoltaics Dataset in China (V3.0) published by Xueyan Zhang and Xin Ma (Science Data Bank, 2025). The dataset records spatial locations, construction years, installed capacity (MW), and 7 agricultural types (crop, greenhouse, herbal, tea, livestock, fishery, forestry) of agrivoltaic stations in vector format. Since the original data are at project level, we aggregated by "Year-Province-City-Type" to obtain annual newly added capacity totals for 370 prefecture-level cities from 2010 to 2022. Areas were estimated by multiplying the number of projects in each aggregated group by an approximate coefficient of 0.02 km² per project. This coefficient is derived from a random sample of 50 projects whose land-use approval documents were publicly accessible. The estimated area data are used for auxiliary descriptive purposes only and do not serve as the basis for any core conclusions of this study.

## 2.2 Methods

(1) Temporal and spatial statistics: Annual summation and Pareto ranking (Top 20) were used.

(2) Random Forest Regression: To identify driving factors. Input features included normalized year, one-hot encoded 7 types, and dummy variables for the top 10 provinces. The target was annual new capacity. An 80/20 train-test split was used, with $R^2$ and MAE evaluating performance.

(3) Comprehensive Benefit Index (CBI): Based on 2020-2022 data, four dimensions—Carbon reduction (0.8 kt/MW), Elderly employment (estimated based on area), Youth employment (estimated based on area), and Economic output (2 million CNY/MW)—were normalized via Min-Max and weighted (0.25:0.30:0.30:0.15) to synthesize a final score. It must be emphasized that the employment dimensions in CBI rely on area estimates; therefore, the CBI results should be interpreted as illustrative rather than definitive.

# 3 Experimental Results

## 3.1 Annual Evolution of Capacity and Area

Fig. 1 shows that new capacity followed a "steep rise then high-level fluctuation" path. The incubation period (2010-2014) averaged <1,000 MW/year, followed by an explosive phase (2015-2017) with >40% annual growth, peaking at 21,937.2 MW in 2017. In 2018-2019, capacity dropped to about 12,000 MW due to subsidy cuts and grid constraints, then stabilized at 15,000-17,000 MW during 2020-2022. Analysis: The 2017 peak is closely related to the dense implementation of "photovoltaic poverty alleviation" policies during the 13th Five-Year Plan, while the "531 New Policy" in

2018 caused short-term contraction, followed by gradual recovery as the market adapted to grid parity.

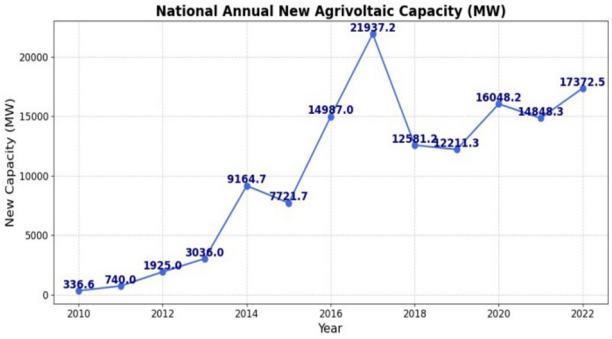



**Fig. 1.** Annual Newly Installed Agrivoltaic Capacity in China (MW)

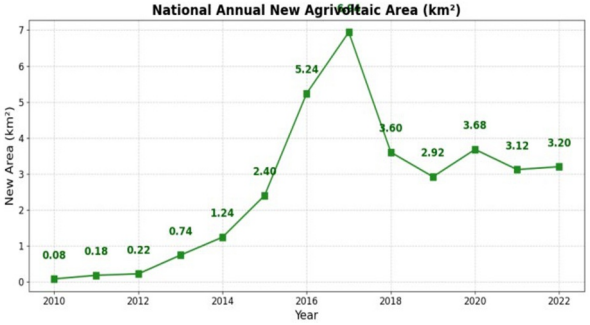



**Fig. 2.** Annual Newly Installed Agrivoltaic Area in China (km²)

Correspondingly, new area peaked at 6.94 km² in 2017 (Fig. 2), but by 2022 area (3.20 km²) shrank by 54% while capacity shrank only 21%. The divergence between area and capacity changes may be related to evolving land-use conditions in project siting, though the specific mechanisms require further investigation with additional data

## 3.2 Type Structure and Top 20 City Agglomeratio

Table 1 shows that Crop (68,720.7 MW) and Fishery (48,199.4 MW) jointly account for 85.7% of the total. Forestry, Livestock, and Greenhouse together account for ~11%, while Herbal and Tea are below 1%. Analysis: Crop and fishery dominate because open fields and fish ponds require low transformation costs and offer quick returns. "PV+aquaculture" also reduces water evaporation and improves breeding efficiency, forming positive economic feedback. The extremely low shares of herbal and tea may be due to their high sensitivity to shading; future breakthroughs in transparent PV modules could change this.

**Table 1.** Cumulative Installed Capacity by Agricultural Type (MW)

| Type | Capacity | Share (%) |
|---|---|---|
| Crop | 68720.7 | 52.8 |
| Fishery | 48199.4 | 37.0 |
| Forestry | 6717.5 | 5.2 |
| Livestock | 5538.0 | 4.3 |
| Greenhouse | 3272.3 | 2.5 |
| Tea | 244.8 | 0.2 |
| Herbal | 217.0 | 0.2 |
| ==Total | 130109.7 | 100 |

Fig. 3 reveals spatial polarization: the top 20 cities each exceed 1,690 MW, with Qianxinan AP (5,620 MW), Qingyuan (4,153 MW), and Anshun (3,380 MW) ranking top three. These cities are mostly in the mountainous southwest or coastal south, benefiting from abundant solar radiation, water areas, and strong agricultural bases. Analysis: Qianxinan AP benefits from low-latitude, high-altitude solar conditions, coupled with local government support for land transfer, making it a hotspot.

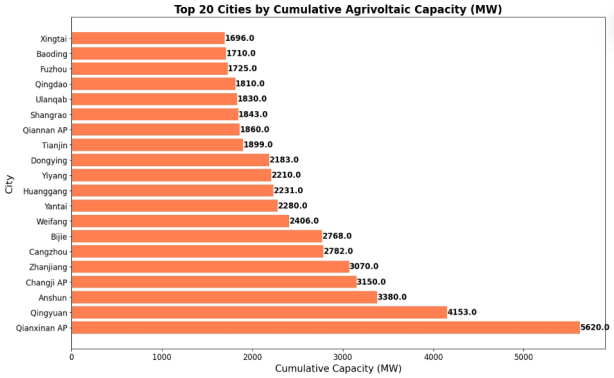



**Fig. 3.** Top 20 Prefecture-Level Cities by Cumulative Installed Capacity (MW)

### 3.3 Driving Factor Analysis of Installed Capacity

In Fig. 4 RF model yields a test $R^2$ of -0.224 and an MAE of 106.49 MW. This negative $R^2$ indicates that the model, using only internal features (normalized year, type dummies, and province dummies), fails to capture the core variance in capacity fluctuations. This is not a methodological failure but rather a meaningful empirical finding: it demonstrates that agrivoltaic capacity installation is primarily driven by external factors—such as feed-in tariffs, subsidy policies, PV module costs, and grid connection conditions—rather than by time trends or type structures alone.

Consequently, the feature importance ranking presented below should be interpreted with caution. It reflects relative contributions only among the limited set of internal features included in this model, not a causal ranking of true driving factors. With this caveat, the ranking shows that Normalized Year (0.444) ranks first, Fishery (0.113)

and Crop (0.101) rank second and third, and provincial features (e.g., Hebei 0.050, Shandong 0.046) reflect regional policy implementation differences.

The negative $R^2$ also suggests that future work must incorporate GDP, sunshine hours, and provincial subsidy policy documents to achieve predictive power.

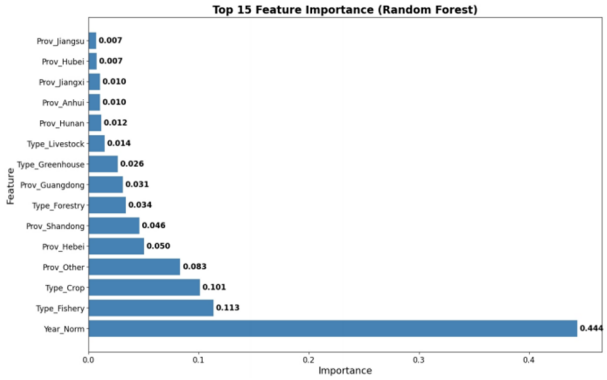



**Fig. 4.** RF Feature Importance Top 15

### 3.4 Regional Comprehensive Benefit Index Ranking

Fig. 5 shows that Qianxinan AP tops with a perfect score of 1.000, with both capacity (4,120 MW) and estimated area (0.92 km²) far ahead, indicating comprehensive pull effects. Cangzhou (0.436), Anshun (0.403), and Bijie (0.392) form the second tier.

The CBI ranking does not perfectly match the capacity ranking (e.g., Qingyuan ranks 2nd in capacity but 10th in CBI) because the index incorporates "employment per unit area", giving compensatory credits to cities with larger estimated areas. However, since the area data used in CBI are estimates, these rankings should be viewed as indicative rather than definitive. Low-ranking cities (e.g., Shijiazhuang 0.145) may benefit from refined area measurements in future studies.

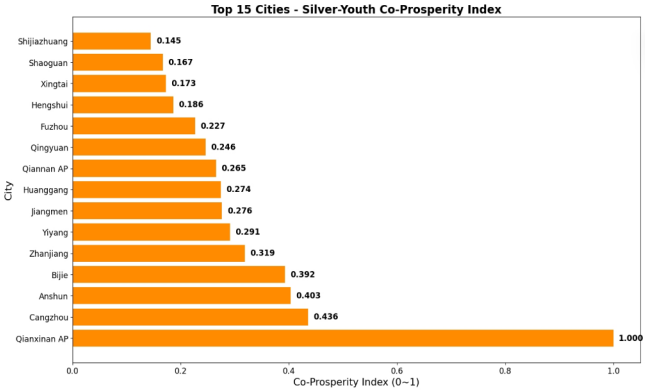



**Fig. 5.** Prefecture-Level Cities by Comprehensive Benefit Index

## 4 Conclusion and Future Work

Based on panel data from 370 prefecture-level cities during 2010-2022, through temporal statistics, type structure analysis, Random Forest driving factor identification, and CBI construction, we conclude that: China's agrivoltaic capacity experienced a three-phase "incubation-explosion-fluctuating adjustment", with 2017 as a turning point, after which the industry entered a period of scale stabilization and quality improvement; "Crop+Fishery" contributed 85.7% of cumulative capacity, and Qianxinan AP, Qingyuan, and Anshun are spatial hotspots; Time trend and fishery/crop types show relatively high importance among internal features, but the model's negative $R^2$ indicates that external policy and socioeconomic variables are indispensable and must be included in future analyses; The CBI ranks Qianxinan AP top, and capacity ranking differs from benefit ranking, suggesting that land-use efficiency and social-environmental outputs deserve more attention, though the CBI results should be interpreted with caution due to the use of estimated area data.

Future research can deepen in three directions: First, integrating nighttime light (GDP proxy), sunshine duration, and provincial subsidy policy counts to improve the explanatory power of predictive models; Second, using GIS analysis on the original SHP data to precisely calculate actual land occupation for each project, thereby replacing the estimated areas used in this study; Third, conducting life-cycle economic and environmental comparisons across different agrivoltaic types to inform differentiated subsidy policies. Additionally, the format of this paper should be carefully cross-checked against the journal's official template to ensure strict adherence to all formatting guidelines, including font specifications, section numbering, table layouts, and reference styles.

## References

1. Liao B, Qi Y, Fu W, et al. Current status and future trends in China’s photovoltaic agriculture development[J]. Sustainability, 2025, 17(19): 8625. DOI: 10.3390/su17198625.
2. Zhang L, Yang Z, Wu X, et al. Open-field agrivoltaic system impacts on photothermal environment and light environment simulation analysis in Eastern China[J]. Agronomy, 2023, 13(7): 1820. DOI: 10.3390/agronomy13071820.
3. Geng X, Liu H, Bao E, et al. Light environment heterogeneity and agricultural yield assessment of photovoltaic farmland with tracking agrivoltaic array: Field experiments and numerical simulations[J]. Sustainability, 2026, 18(10): 5164. DOI: 10.3390/su18105164.
4. Wu Zhaoxue, Yuan Tianyun, Bao Encai, et al. Effects of photovoltaic module density on micro-environment and sweet potato yield in agrivoltaic systems[J]. Transactions of the Chinese Society of Agricultural Engineering, 2025, 41(22): 256-264. DOI: 10.11975/j.issn.1002-6819.202505012.
5. Zhang X, Ma X. Vectorized agrivoltaics dataset in China from 2010 to 2022[J]. Scientific Data, 2026, 13: 116. DOI: 10.1038/s41597-025-06305-w.
6. Zhu B, Yang C, Dai J, et al. $R_2FD_2$: Fast and robust matching of multimodal remote sensing images via repeatable feature detector and rotation-invariant feature descriptor[J]. IEEE Transactions on Geoscience and Remote Sensing, 2023, 61: 1-15. DOI: 10.1109/TGRS.2023.3264610.

7. Tu H, Zhu Y, Han C. RI-LPOH: Rotation-invariant local phase orientation histogram for multi-modal image matching[J]. Remote Sensing, 2022, 14(17): 4228. DOI: 10.3390/rs14174228.
8. Zhang S, Luo B, Liu J, et al. GLIFT: A global-to-local invariant feature transformation method for multi-modal remote sensing image matching[J]. IEEE Transactions on Geoscience and Remote Sensing, 2025. DOI: 10.1109/TGRS.2025.3599445
9. Geng Z, Yang B, Pi Y, et al. MIRRIFT: Multimodal image rotation and resolution invariant feature transformation[J]. IEEE Transactions on Geoscience and Remote Sensing, 2025, 63: 1-16. DOI: 10.1109/TGRS.2025.3554642.
10. Time A, Gomez-Casanovas N, Mwebaze P, et al. Conservation agrivoltaics for sustainable food-energy production[J]. Plants, People, Planet, 2024, 6(3): 558-569. DOI: 10.1002/ppp3.10481.

**Open Access** This chapter is licensed under the terms of the Creative Commons Attribution-NonCommercial 4.0 International License (http://creativecommons.org/licenses/by-nc/4.0/), which permits any noncommercial use, sharing, adaptation, distribution and reproduction in any medium or format, as long as you give appropriate credit to the original author(s) and the source, provide a link to the Creative Commons license and indicate if changes were made.

The images or other third party material in this chapter are included in the chapter's Creative Commons license, unless indicated otherwise in a credit line to the material. If material is not included in the chapter's Creative Commons license and your intended use is not permitted by statutory regulation or exceeds the permitted use, you will need to obtain permission directly from the copyright holder.

